

*Dedicated to Academician Professor Dr. Emil Burzo on His 80<sup>th</sup> Anniversary*

## NANOCRYSTALLINE MAGNETITE - $\text{Fe}_3\text{O}_4$ PARTICLES SYNTHESIZED BY MECHANICAL MILLING

T.F. MARINCA<sup>1</sup>, H.F. CHICINAȘ<sup>1</sup>, B.V. NEAMȚU<sup>1</sup>, F. POPA<sup>1</sup>,  
O. ISNARD<sup>2,3</sup>, I. CHICINAȘ<sup>1,\*</sup>

**ABSTRACT.** Nanocrystalline magnetite –  $\text{Fe}_3\text{O}_4$  has been synthesized in nanocrystalline state by mechanical milling of well crystallized magnetite samples obtained by heat treatment of a stoichiometric mixture of iron and hematite. Upon increasing the milling time, the mean crystallite size of magnetite is diminishing. After only 5 minutes of mechanical milling the crystallites are 110 nm. The milling up to 120 minutes leads to a continuous reduction of crystallites size up to 8 nm. The mechanical milling process induces strains into the lattice and the lattice strains increase drastically in the first 60 minutes of milling, after that a saturation of lattice strains is noticed. During milling a contamination of the powder with elemental iron occurs for milling times larger than 30 minutes. A decrease of the saturation magnetisation is noticed upon increasing the milling time and the decrease is associated with the structural disorder and defects that are induced into the material during milling. A tendency of the magnetisation to become unsaturated is also noticed and it is related to canted spins effect.

**Keywords:** *mechanical milling, magnetic material, ferrite, magnetite, nanocrystalline.*

### INTRODUCTION

The iron oxides are of interest both for fundamental research and applicative research and are used in various fields of industry [1-3]. Among the iron oxides, the magnetite -  $\text{Fe}_3\text{O}_4$  is probably the most studied nowadays. The magnetite crystallizes in

---

<sup>1</sup> *Materials Science and Engineering Department, Technical University of Cluj-Napoca, 103-105, Muncii Avenue, 400641 Cluj-Napoca, Romania*

<sup>2</sup> *Université Grenoble Alpes, Inst NEEL, F-38042 Grenoble, France*

<sup>3</sup> *CNRS, Institut NEEL, 25rue des martyrs, BP166, F-38042 Grenoble, France*

\* *Corresponding author e-mail: ionel.chicinas@stm.utcluj.ro*

cubic spinel structure from the space group Fd-3m. Typically, as almost all of the soft ferrites, the magnetite is ferrimagnetic having the Néel point at about 585 °C. The ferrimagnetism of the magnetite derives from the arrangement of the Fe<sup>2+</sup> and Fe<sup>3+</sup> cations into the spinel cubic structure that allows two type of positions: tetrahedral and octahedral. The Fe<sup>2+</sup> cations and half of Fe<sup>3+</sup> cations are positioned in the octahedral positions. The other half of Fe<sup>3+</sup> cations are positioned in the tetrahedral positions. The octahedral positions create a magnetic sublattice aligned antiparallel to the other magnetic sublattice which is formed by the cations from tetrahedral positions [4].

The synthesis of the magnetite particles in nanocrystalline/nanosized state is nowadays a very challenging subject of research due to the large range of new potential applications, such as magnetic refrigeration, magnetic storage systems, magnetic separation, magnetic hyperthermia and cancer therapy [5-8]. There are several synthesis routes that can be used for obtaining magnetite particles in the nanocrystalline/nanosized state: solvothermal [9], co-precipitation [10], hydrothermal [11] or mechano-synthesis [12]. Among these routes, the mechano-synthesis is one of the most versatile approaches, which can be used for the synthesis of nanocrystalline magnetite particles and also magnetite nanoparticles. The nanocrystalline magnetite and magnetite nanoparticles can be obtained using a relatively large range of precursors.

The present paper investigates the structural and magnetic evolution of magnetite powder, obtained from iron and hematite by heat treatment, during mechanical milling processing.

## EXPERIMENTAL

Iron and hematite ( $\alpha$ -Fe<sub>2</sub>O<sub>3</sub>) powders have been used for the synthesis of the magnetite – Fe<sub>3</sub>O<sub>4</sub> powder in nanocrystalline state. The first step of the synthesis consists in homogenising the iron and hematite powders in a Turbula type apparatus for 15 minutes. After that, the stoichiometric powder mixture has been heat treated at 870 °C for 4 h in argon atmosphere (in order to avoid the supplementary oxygen that can be provided by air). The second step consists in the mechanical milling of the magnetite powder obtained by heat treatment. A Fritsch high energy planetary ball mill, model Pulverisette 6, was used for the mechanical milling process. The mechanical milling process has been carried out in argon atmosphere and tempered steel vial and balls were used. A 350 rpm rotational speed was set. The milling process was carried out using a ball to powder mass ratio of 20:1.

An INEL Equinox 3000 diffractometer that works in reflection mode has been used for structural investigation of the powder. The X-ray diffraction patterns have been recorded in angular range of 2 theta = 20-110° using CoK<sub>α</sub> radiation. The mean crystallite size and lattice strain were determined by Williamson-Hall method [13].

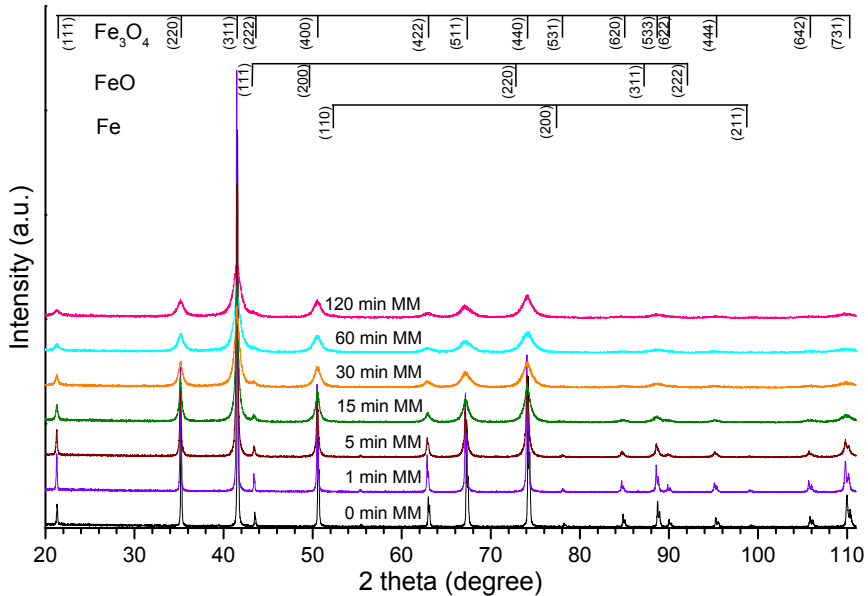
The magnetisation curves at room temperature have been recorded using extraction sample method in a continuous magnetic field up to 9 T. The saturation magnetisation values have been obtained according to the law of approach to saturation:

$$M = M_S \left( 1 - \frac{a}{H} - \frac{b}{H^2} \right) + \chi H \quad (1)$$

The saturation magnetization values were obtained from  $M=f(1/H^2)$  plots from the region of high external magnetic field,  $\mu_0 H \geq 6$  T.

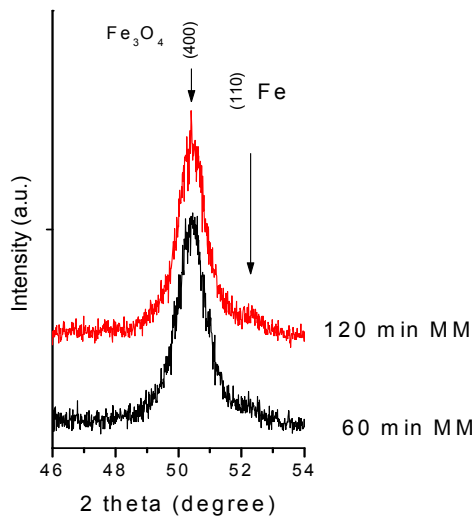
## RESULTS AND DISCUSSION

Figure 1 presents X-ray diffraction patterns of the Fe<sub>3</sub>O<sub>4</sub> samples milled for 0, 1, 5, 15, 30, 60 and 120 minutes. As reference, in the figure are given beside the peaks position of the iron and magnetite, the peaks position for the wüstite phase-FeO. This last oxide is encountered during processing Fe and magnetite. The JCPDS files no. 06-0696 for Fe, no. 19-0629 for Fe<sub>3</sub>O<sub>4</sub> and 06-0615 for FeO have been considered.



**Fig. 1.** X-ray diffraction patterns of the Fe<sub>3</sub>O<sub>4</sub> samples milled for 0, 1, 5, 15, 30, 60 and 120 minutes.

The un-milled sample (sample obtained by heat treatment), marked in the figure as 0 min MM presents only the peaks characteristics for the cubic spinel structure of the magnetite. The same Bragg reflections are observed also for the samples milled up to 60 minutes. In the patterns of the samples milled for 60 and 120 minutes a new Bragg peak can be observed. This peak is assigned to the elemental iron, which is provided by powder contamination during milling. This is a well-known phenomenon that occurs during processing powder by mechano-synthesis route [14, 15]. In the case of milling ferrites the contamination is more pronounced due to the very abrasive characteristic of these materials [15]. In the figure 2 is presented a detail of X-ray diffraction patterns of the  $\text{Fe}_3\text{O}_4$  samples milled 60 and 120 minutes in the  $2\theta$  range where the elemental Fe most intense peak ((110) line) is visible.



**Fig. 2.** Details of X-ray diffraction patterns of the  $\text{Fe}_3\text{O}_4$  samples milled 60 and 120 minutes in the  $2\theta$  range where the Fe most intense peak is visible.

Upon increasing the milling time it can be noticed that the magnetite peaks become larger as compared to the magnetite un-milled sample. This is assigned, on the one hand, to the crystallite size refinement and on the other hand to the internal stresses induced in the samples by mechanical milling process [15]. In the figure 3 is shown the evolution of the mean crystallite size as a function of milling time for the  $\text{Fe}_3\text{O}_4$  milled samples. One can observe that, for short milling times, the magnetite becomes nanocrystalline. After only 5 minutes of milling the mean crystallite size is about 110 nm. By increasing the milling duration at 15 minutes, the mean crystallites size is reduced down to 22 nm. At the final milling duration

the mean crystallites size is about 8 nm. It can be also observed that after 30 minutes of milling, the mean crystallite size variation is lower, from 11 to 8 nm. This is in agreement with the early reported results that show a saturation of the crystallites reduction at a certain milling time [14].

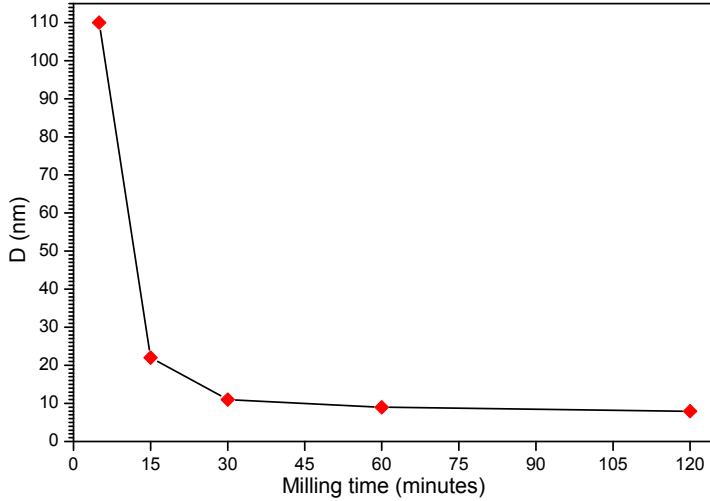


**Fig. 3.** Evolution of the mean crystallite size versus milling time for the  $\text{Fe}_3\text{O}_4$  milled samples.

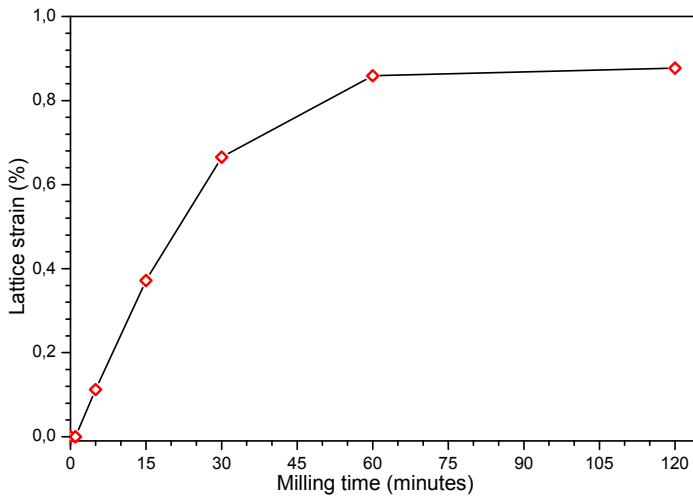


**Fig. 4.** Evolution of the lattice strain versus milling time for the  $\text{Fe}_3\text{O}_4$  milled samples.

Figure 4 presents the evolution of the lattice strain as a function of milling time for the  $\text{Fe}_3\text{O}_4$  milled samples. Upon increasing the milling time the lattice strains increase. In the first half of the milling process, durations up to 60 minutes, a rapid increase of the lattice strain is noticed. After this, in the second half of the milling process a saturation of the lattice strain is attained. The repeated fragmentation and cold welding processes lead to the appearance of the lattice strains [14].

Magnetisation curves recorded at 300 K for the  $\text{Fe}_3\text{O}_4$  milled samples in a magnetic field up to 9 T are presented in the figure 5. It can be noticed that up to 5 minutes of milling the shape and values of the magnetisation are almost unchanged, suggesting that the mechanical milling has a very slight influence above this magnetic characteristic for this milling durations. Further increase of the milling time leads to a significant change of the magnetization. It can be observed that the values of the magnetisations decrease. Also, it is observed that, the magnetisation tends to become unsaturated. This phenomenon is more visible for the samples milled for 60 and 120 minutes. The tendency of the magnetisation to become unsaturated is associated with spin canted effect and other surface effects such as disordered magnetic shell structure [15, 16].

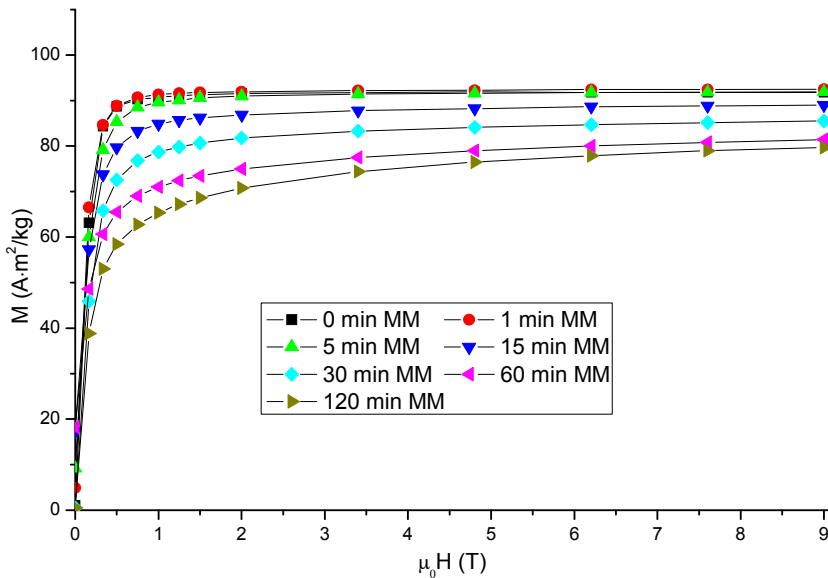
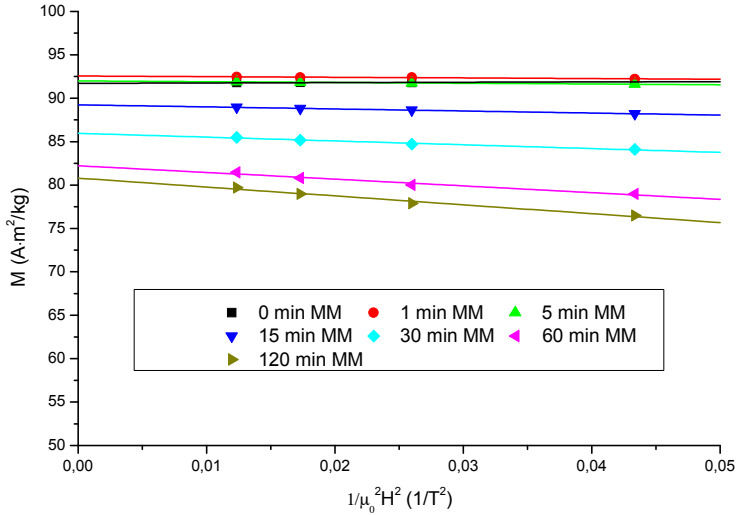
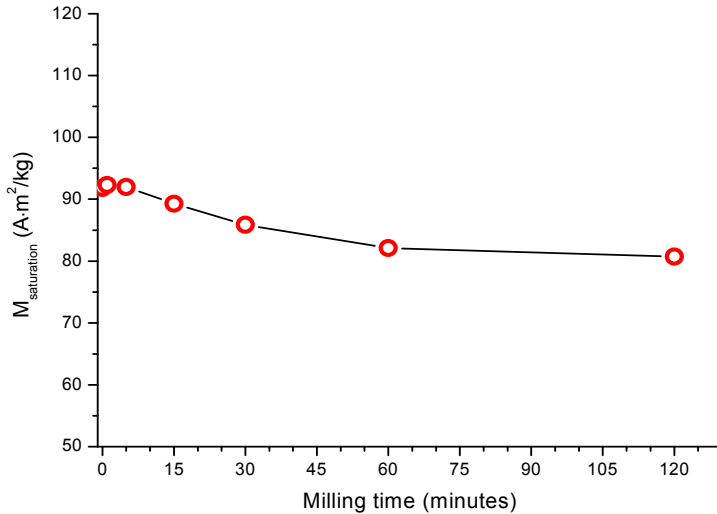


Fig. 5. Magnetisation curves recorded at 300 K for the  $\text{Fe}_3\text{O}_4$  milled samples.



**Fig. 6.**  $M=f(1/H^2)$  plots of the Fe<sub>3</sub>O<sub>4</sub> milled samples.

In order to determine the saturation magnetisation of the magnetite samples the  $M$  versus  $(1/(\mu H)^2)$  has been plotted. The  $M(1/(\mu H)^2)$  plots are presented in the figure 6. It can be observed that in the high-field region the  $M$  versus  $(\mu H)^2$  plots have good linearity and the extrapolation to zero represents the values of the saturation magnetization.



**Fig. 7.** Evolution of the saturation magnetisation of the Fe<sub>3</sub>O<sub>4</sub> milled samples versus milling time.

The value of saturation magnetisation as resulted from the  $M=f(1/(\mu H)^2)$  plots as a function of milling time is shown in the figure 7. It can be observed that the saturation magnetisation decreases upon increasing the milling time. In the case of the un-milled samples (0 minutes MM) the saturation magnetisation is about  $91.8 \text{ A}\cdot\text{m}^2/\text{kg}$  and in the first 5 minutes of milling is almost constant. The value of the saturation magnetisation is very close to the one reported for the magnetite in reference [4] of about  $92 \text{ A}\cdot\text{m}^2/\text{kg}$ . After that, a decrease is observed, the saturation magnetisation decreases up to  $80.7 \text{ A}\cdot\text{m}^2/\text{kg}$  upon increasing the milling time up to 120 minutes. The magnetisation decreased with about 11 % upon increasing the milling time from 0 to 120 minutes. The decrease of the saturation magnetisation is caused by the structural disorder and defects induced into the samples by high energy ball milling. These defects can be dislocations, vacancies, cations inversion, spin canted or surface spin disorder [15, 16]. If is taken into account a full inverse spinel ferrite (all the  $\text{Fe}^{2+}$  cations are located in octahedral sites) the net magnetic moment for a magnetite molecule is  $3.8 \mu\text{B}$ . Resulting thus that the  $\text{Fe}^{2+}$  cations possess also a net magnetic moment of  $3.8 \mu\text{B}$ . This is very close to the calculated one which is  $4 \mu\text{B}$ . The net magnetic moment of the magnetite molecule decreases upon milling the sample for 120 minutes at about  $3.35 \mu\text{B}$ . This suggests a large particles specific surface of the particles (very fine particles), that give rise to large amount of cations that have canted spins.

## CONCLUSIONS

The nanocrystalline magnetite powder has been successfully obtained by mechanical milling of the well crystallised samples synthesised by heat treatment of a stoichiometric mixture of iron and hematite. The mean crystallite size decreases upon increasing the milling time and in the same time the lattice strains that are induced into the sample increases. A powder contamination with elemental iron provided by milling bodies was noticed. The magnetisation of the samples decreases upon increasing milling time due to the several causes such as structural defects and structural disorder, internal stresses or surface effects. The magnetisation tends to become unsaturated for long milling time as a result of spin canted effect.

## ACKNOWLEDGEMENTS

This paper was supported by the Post-Doctoral Programme POSDRU/159/1.5/S/137516, project co-funded from European Social Fund through the Human Resources Sectorial Operational Program 2007-2013.



## REFERENCES

1. R.M Cornell, U. Schwertmann, "The iron oxides", Wiley-VCH Verlag, KGaA, Weinheim, 2003.
2. A.K. Gupta, M. Gupta, *Biomaterials*, 26, 3995 (2005).
3. N.M. Deraz, A. Alarifi, *Ceram. Int.*, 38, 4049 (2012).
4. B.D. Cullity, C.D. Graham. "Introduction to Magnetic Materials", 2nd edition, IEEE Press & Wiley, New Jersey, 2009.
5. D. Wilson, M.A. Langell, *Appl. Surf. Sci.*, 303, 6 (2014).
6. P. Panneerselvam, N. Morad, K.A. Tan, *J. Hazard. Mater.*, 186, 1608 (2011).
7. K. Hayashi, W. Sakamoto, T. Yogo, *J. Magn. Magn. Mater.*, 321, 450 (2009).
8. M. Fang, V. Ström, R.T. Olsson, L. Belova, K.V. Rao, *Nanotechnology*, 23, 145601 (2012).
9. C. Li, Y. Wei, A. Liivat, Y. Zhu, J. Zhu, *Mater. Lett.*, 107, 23 (2013).
10. B. Peeples, V. Goornavar, C. Peeples, D. Spence, V. Parker, C. Bell, D. Biswal, G.T. Ramesh, A. K. Pradhan, *J. Nanopart. Res.*, 16, 2290 (2014).
11. X. Wu, J. Tang, Y. Zhang, H. Wang, *Mater. Sci. Eng., B*, 157, 81 (2009).
12. G.F. Goya, *Solid State Commun.*, 130, 783 (2004).
13. G.K. Williamson, W.H. Hall, *Acta Metall.*, 1, 22 (1953).
14. C. Suryanarayana, "Mechanical Alloying and Milling", Marcel Dekker, New York, 2004.
15. T.F. Marinca, I. Chicinaş, O. Isnard, V. Popescu, *J. Am. Ceram. Soc.*, 96, 469 (2013).C.N.
16. Chinnasamy, A. Narayanasamy, N. Ponpandian, K. Chattopadhyay, H. Guérault, J.-M. Grenèche, *Journal of Physics: Condensed Matter*, 12, 7795 (2000).

